Civil Engineering and Architecture 13(6): 4401-4418, 2025 http://www.hrpub.org
DOI: 10.13189/cea.2025.130621

Optimizing Construction Safety for Segmental Bridges: ANSYS-Based Simulation Assessment of Stress-Strain Behavior under Critical Construction Stage

N. J. Jain*, **S. Sangita Mishra, Shrikant Charhate**

Amity School of Engineering and Technology, Amity University Mumbai, Maharashtra, India

Received July 12, 2025; Revised September 24, 2025; Accepted October 21, 2025

Cite This Paper in the Following Citation Styles

(a): *[1] N. J. Jain, S. Sangita Mishra, Shrikant Charhate , "Optimizing Construction Safety for Segmental Bridges: ANSYS-Based Simulation Assessment of Stress-Strain Behavior under Critical Construction Stage," Civil Engineering and Architecture, Vol. 13, No. 6, pp. 4401 - 4418, 2025. DOI: 10.13189/cea.2025.130621.*

(b): *N. J. Jain, S. Sangita Mishra, Shrikant Charhate (2025). Optimizing Construction Safety for Segmental Bridges: ANSYS-Based Simulation Assessment of Stress-Strain Behavior under Critical Construction Stage. Civil Engineering and Architecture, 13(6), 4401 - 4418. DOI: 10.13189/cea.2025.130621.*

Abstract Mitigating the risk of catastrophic failures of bridges during the construction stage of precast segmental structures remains a critical challenge for civil engineers across the world. Recent incidents have underscored the vulnerability of these complex bridge structures in their incomplete state where the traditional design checks often seemed deficient. This research addresses those gaps by proposing and demonstrating a robust stress and strain based analysis framework specifically targeting the construction phase of the bridge structure. It utilized an advanced 3D Finite Element Analysis with a high simulation tool called ANSYS to develop a highly detailed 40m long and 25m wide six lane full scale model of a representative precast PSC segmental structure. The core focus is to simulate the realistic application of critical construction stage loadings by meticulously tracking the stress and strain distribution patterns, along with their magnitudes throughout the key structural elements (segments, joints, temporary supports, bearings, etc.) at each simulated erection step. The model aims to identify the potential overstress conditions within the M55 concrete grade structure before they are ready to manifest in the real world scenario. The ANSYS based simulations provided unprecedented insights into the stress behaviour of segmental bridge with a maximum principal stress of 25.3 N/mm^2 observed near the support segments, and the strain behavior evolves during the inherently unstable construction sequence with the value of strain reaching up to 0.0024, revealing the critical zones susceptible to excessive deformation or cracking. The findings demonstrate that strain based monitoring within a sophisticated 3D FEA approach offers a powerful predictive tool for engineers, whereas the conventional stress or displacement limits provide a more sensitive indicator of structural distress under the unique and often underestimated loads present only during construction.

Keywords Segmental Bridge, Strain Behaviour, Construction Loads, Construction Safety, Finite Element Analysis

1. Introduction

Precast segmental bridge construction has revolutionized infrastructure development through accelerated erection and enhanced quality control. The evolution of precast segmental bridge construction in India has been well documented by the researcher in 2021 [1] who traced the transition from conventionally adopted cast-in-situ methods to an advanced/innovative system of precast segmental techniques for the elevated corridors having long-span viaducts. The literature also identifies challenges like geometry control, joint integrity, and quality assurance during the precast segment handling including transportation and erection. The study concludes that the precast segmental bridge not only accelerates the project timelines but also enhances the construction safety and durability making it a strategic choice for development of the urban bridge infrastructure in India [2]. However, this innovative advancement remains vulnerable to catastrophic failures during the transient construction phases, where structural systems exhibit incomplete stiffness and unconventional load paths. It is very necessary to notice the failures occur across the globe during the construction stages, whether these structures are dealing with the national highways or metros irrespective of their use [3]. The bridge construction failures during the erection/construction stages, especially in case of precast segmental bridges, have raised serious concerns about safety and quality controls in the recent years. Figure 1 shows a collective collage of several incidents across India, such as those in Haryana, West Bengal, Varanasi, and Gurgaon, which have shown how vulnerable these structures can be even after high supervision and technical checks followed yet leading to the total collapse during the construction [4-6]. These accidents happened during the girder/segment launching stage, concrete crushed due to high compression in the soffit, and hogging failure pattern is also observed in some cases or due to the failure of temporary supporting systems. Such situations not only risk the human lives but also delay the infrastructure projects' outcome with a huge impact on the financial factors. Learning from these kinds of failures is very important to improve the design practices, construction planning, and workmanship followed by the technical checks with site monitoring of the crucial parts for the future bridge works. This research, on the other hand, proposed a more complex approach for the analysis and design of such complex structures rather than the linear static or linear dynamics analysis.

The study done by the researcher in 1979 [7] mainly focuses on identifying the critical quality control events in concrete bridge construction for enhancing the structural reliability and its service life. It highlights the applied innovations for formwork design, concrete mix, vibration techniques and curing methods, which further offer a step-by-step framework to improve the site execution. The study presents a realistic approach for improving bridge durability by further addressing challenges like material inconsistencies, inadequate labor training, and poor construction management/methodology. However, the study lacks performance based data analysis with the application of digital monitoring tools, bigger environmental considerations, and also the key factors which are affecting the overall strength of concrete due to such lack, which may trigger a structural collapse. A typical study aims to predict full load response curve upto failure with the help of nonlinear flexural behavior of prestressed concrete box girder bridges using a finite element approach [8]. The innovative use of the NONLACS program provided with a more accurate simulation of deflection patterns, stress distributions and load capacities by incorporating anisotropic shell elements, tension stiffening for cracked concrete. Results showed a close correlation with experimental findings for validating the method as a reliable and cost effective alternative to the physical testing. Figure 2 shows the study focuses on the strain behaviour of the HT strands with dual cell and single cell bog segments [9]. However, the study simplifies certain aspects particularly concrete stress behavior post cracking and by assuming ideal bond conditions but lacking the strain for the concrete.

Figure 1. Under construction precast segmental bridge failures [4-6]

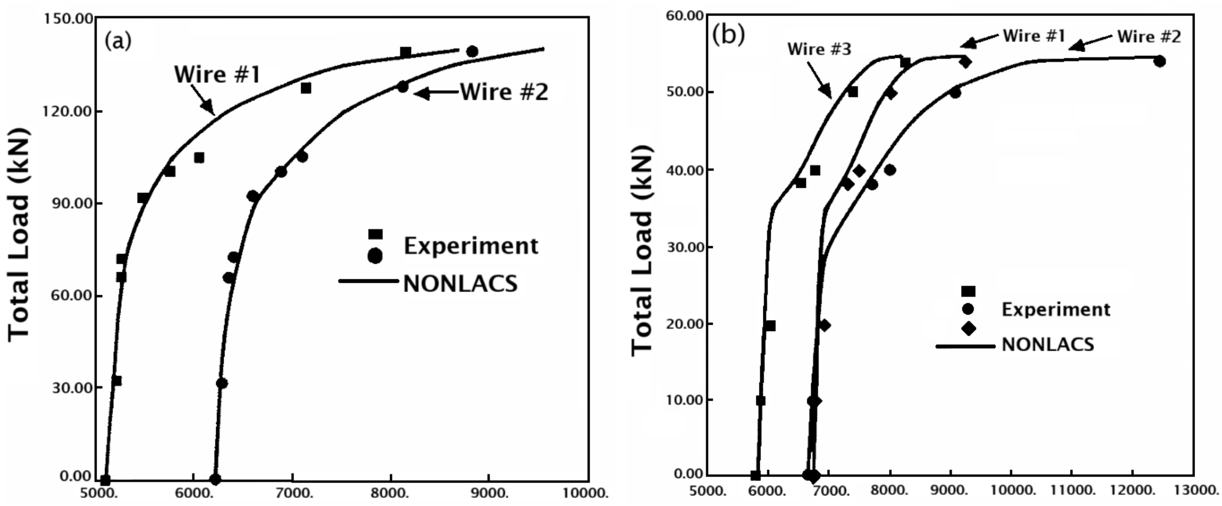

(a) Two Cell Box (b) Single Cell Box

Figure 2. Strain in HT Strands [9]

The study does not cover the effects of shear, torsion, or dynamic loads, which are essential for comprehensive assessment in real world highway bridges. These limitations highlight the need for further research into multi axial behavior and time dependent strain effects under varied loading scenarios. The researchers propose a study regarding a design of a 2000 m long post-tensioned segmental bridge near the Andaman and Nicobar Islands using M60 grade of concrete and Fe415 steel as per IRC:21-2000 [10,11]. A parabolic cable profile with Freyssinet system of 27K-15 (27 strands of 15.2 mm diameter) is adopted, and deck slab analysis is performed using Pigeaud’s method, yielding live load bending moments of 61.75 kN.m for short span and 30.32 kN.m for long span. The prestressing force is calculated using the equation (1) as given below:

$$P = \frac{A_b f Z_b}{Z_b + A_e E} = 59573.64\ kN \tag{1}$$

Final vertical load on elastomeric bearings is around 2443.38 kN, which falls within the safe range as per the IRC:83 [12]. While the study confirms the structural safety and the material efficiency, it lacks the dynamic performance of the structure, where the analysis as per FEM simulation and detailed seismic evaluation is very much needed, which is limiting its applicability to higher complex loading scenarios. A study in [13] recommending the use of longer span continuous bridge structures in modern bridge construction highlights its advantages in structural stability, adaptability and seismic performance. A PSC bridge of 939.44 m as a case example with a longest span of 72m is considered for a balanced cantilever construction with stress monitoring through BIM software and segmental alignment control. However, the study lacks quantitative data, code-based validation and comparative performance analysis, pointing to the exact need of this study for a deeper technical evaluation in the future applications. The researchers aimed to enhance the structural performance and efficiency in the construction of long-span cable-stayed bridge structures. The innovation here is the modular design of a dual steel shell system, which is connected by a PBL (Perfobond Leiste) shear connectors and angle steels, permitting for high prefabrication, reduced on site labor with improved flexural and axial stiffness of the structure. The full scale model testing, along with numerical simulations, validated its superior mechanical behavior, construction feasibility, and compliance with the codal requirements. However, the study highlights limitations such as the concrete void formation, reliance on the precision of fabrications in factory and the need for further/robust research into long term durability and vibration effects in the complex cable arrangements [14].

The researchers propose a study related to the analysis and design of a 35 m multi cell PSC box girder using FE analysis in CSI Bridge software. The study is focusing on the comparative performance of HDPE and Bright Metal sheathing ducts. The results show that HDPE offers a better elongation with lower shrinkage losses and reduced deflection, at midspan which is around 8.08 mm over 8.83 mm respectively, making HDPE more efficient and economical. Final stresses in both cases remained within IRC limits and ultimate strength and shear checks confirmed structural safety for both the cases [15]. However the study does not include dynamic or seismic analysis which is limiting its application to static design conditions. The authors in a study [16] propose the nonlinear behavior of RC beams using the ANSYS. The linear elastic, elasto-plastic and multilinear hardening models are tested under the cracking and the crushing conditions using both discrete and smeared reinforcement patterns. Results show that multilinear compressive models without crushing (for cases 2k and 3p) provide the most realistic load to deflection responses which is closely matching the theoretical predictions. However combining the crushing with plasticity often leads to the early convergence failure, which is highlighting a limitation in ANSYS material handling capabilities. A similar type of study investigates the nonlinear behavior RC and pre-tensioned concrete beams using ANSYS. The study focuses on load to deflection responses, stress distribution and crack propagation under symmetric vertical loading. The pre-tensioned beam exhibited a higher service load range with an ultimate load capacity of 143.6 kN compared to the reinforced beams having capacity of 119.58 kN. The numerical predictions closely matched the theoretical values for the deflection and the stress. Overall the study confirms that ANSYS can effectively simulate real time structural behavior with more accuracy, depending on the refined input modeling and experimental calibration for enhanced reliability [17].

A study [18] evaluates the behavior of a three-span cast-in-situ segmental box girder using MIDAS and STAAD Pro software primarily focusing on the balanced cantilever construction with the time dependent effects. The analysis captures critical stress values and bending moment variations during the construction, after completion and during the service stages. It states that the reversal moment occurs near the support due to early stage cantilever tendons, causing a maximum compressive stresses in the top fibers and the tensile stresses at the bottom fibers. Transient analysis showed that creep induced moment redistribution leads to almost 17–20% reduction in negative moments near the support and a corresponding increment in the positive moments at mid-span over the period of time. Stress checks confirm the safety within AASHTO-LRFD limits at all the stages. However the study assumes ideal boundary conditions and lacks the seismic/dynamic load assessments hence, suggesting the need for more comprehensive simulation for broader application in critical zones.

2. Methodology

Before starting complex simulations, an entire step-by-step process is planned carefully. A systematic workflow is established prior to simulation execution to ensure methodological rigor. This involved developing a comprehensive flowchart shown in Figure 3, delineating all analytical stages from the initial geometry creation to the result validation.

This visual guide showed every critical stage - from building the initial three dimensional model in a 3D-Modelling tool for interpreting the results by simulation analysis. The flowchart clearly explains the following:

- Defining geometry based on preliminary designs (segment sizes, cable paths, temporary supports)
- Assign material properties (concrete behavior, steel reinforcement specs)
- Joint connections set up between segments to segments

Most importantly, it organized how construction loads like Dead Loads (segment self-weight) and SIDL (equipment weight) would be applied at each assembly stage, tracking how loads build up over time. Crucially, it placed strain measurements – like peak strains in concrete and joint stresses – at the centre of the analysis. This directly linked simulation outputs to the construction safety goals.

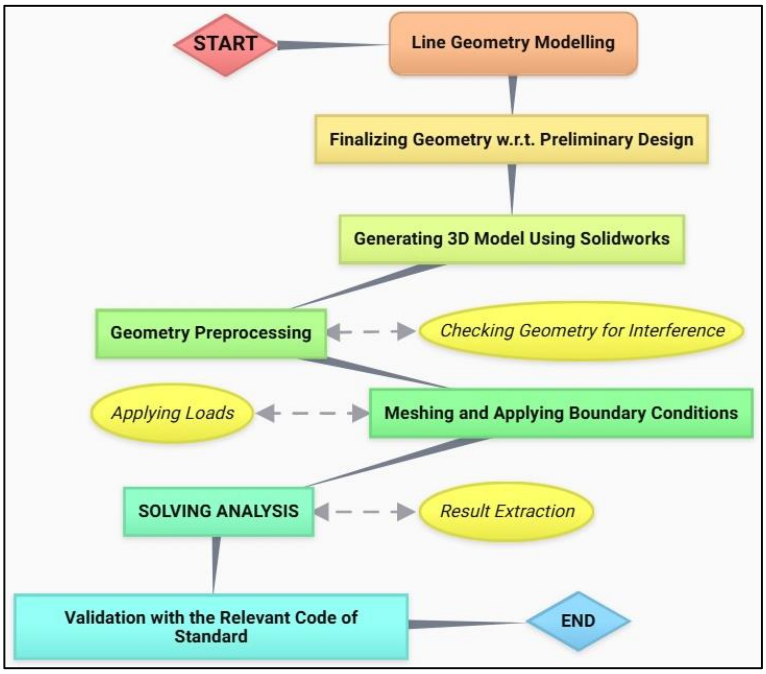

Figure 3. Conceptual Workflow

2.1. Line Geometry Modelling

This phase is the establishment of the digital foundation for any structural simulation. Precise dimensional data based on the preliminary design of structure is translated into a computable format, ensuring all geometric entities which include segment profiling, post-tensioning ducting, and temporary support conditions conform to the construction specifications sequence prior to the analysis. Specifically for the curved bridges or the segmental bridge structure, the line geometry makes it easier for simulation of tendon profiles and to keep a track that how the structure behaves under various forces, making the analysis both practical and reliable. The line geometry modelling was defined using the ANSYS-SpaceClaim by importing the preliminary layout to ensure accurate representation of the span arrangements, tendon curvature profile and the temporary supports conditions. Each tendon profile was parameterized so that the construction stage prestressing application could be simulated sequentially. Present analytical approach not only simplified the curved bridge modelling but also ensured the repeatable alignment with construction stage sequences.

2.2. Finalizing the Geometry w.r.t Preliminary Design

The geometry finalization with respect to the preliminary design and analysis is an important phase in bridge engineering where the conceptual layout is modelled into a practical and analyzable form. At this point of work the dimensions like span length, width of superstructure, thickness of deck slab, bearing positions, temporary support locations, trajectory of the HT strands (tendon bars), curvature, slope nos. of segments, etc…, are finalized based on the structural and the site constraints with the construction based on feasibility and functional requirements. The dimensional accuracy was verified through cross-referencing design tolerance requirements as per the IRC 78, particularly at segment joints and HT-strands anchorage zones, where any geometric deviations would critically influence the stress distributions across the superstructure. Figure 4 shows the geometric dimensions of the bridge structure selected to move forward with the detailed analysis based on the conceptual workflow methodology shown in Figure 3.

The finalized geometry shown in Figure 4 was checked against the dimensional tolerance requirements specified in IRC:78 and IRC SP 87 [19,20]. The segment joint widths, duct spacing and the anchorage zones were verified within the limit of ±5 mm tolerance, as deviations could significantly alter the stress values at transfer. These checks are to ensure the conformity with the practical construction tolerances.

2.3. Generating 3D Model Using SolidWorks

The 3D modelling is done using a tool namely SolidWorks for current study, as the tool offers some ease with the modelling for the conceptualization of the complex models of structural arrangements including the geometry, connections and spatial arrangements. The 3D modelling process of the structure not only enhances the design accuracy but also improves the communication between designing team, construction team, and the approving agency by providing a clear and a realistic view of the structure before the actual construction begins at the site. Figure-5 shows the 3d modelled sketch of the considered geometry. The 3D model from SolidWorks was imported into ANSYS-Workbench for further simulation processing to ensure that the geometric fidelity of the segment profiles and the connections were retained while enabling the finite element meshing and the loading assignment in the analysis.

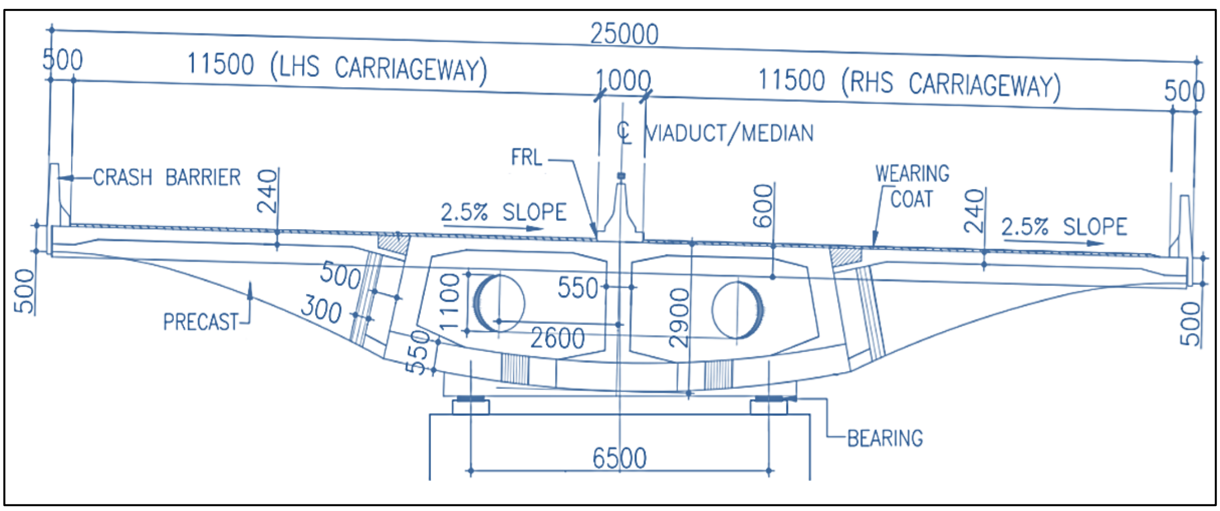

Figure 4. Preliminary Design Based Geometry with Dimensions

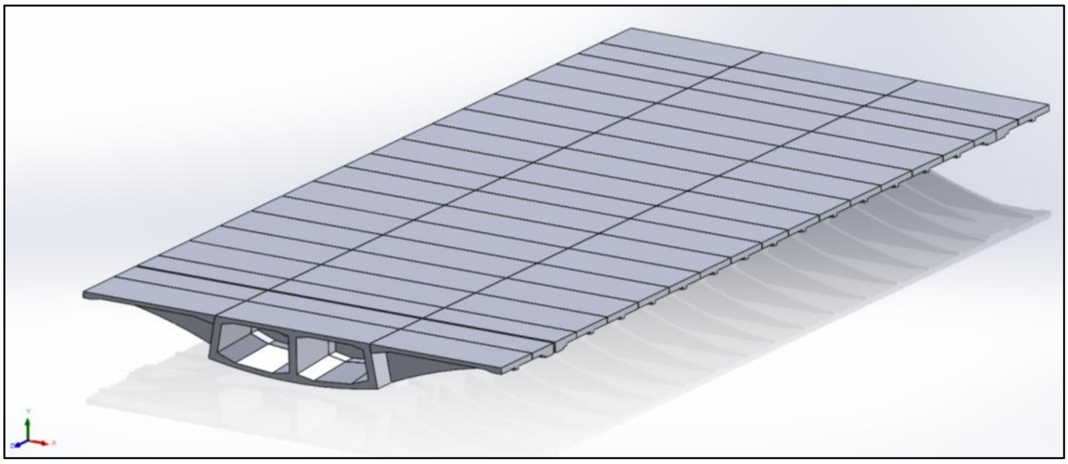

Figure 5. Three Dimensional Modelled Structure

2.4. Geometry Pre-Processing (Checking Geometry for Interference)

Followed by the 3D model generation a comprehensive interference detection was executed within ANSYS-Space Claim tool to eliminate any geometric conflicts prior to the finite element analysis. This is the critical pre-processing phase which involves virtual assembly of all structural components like segment, PSC ducts, temporary supports followed by an automated collision/overlapping detection at the construction stage interfaces, particularly a detailed scrutiny applied to high-risk zones such as tendon duct penetrations through segment webs (with a minimum 8mm clearance verified).

The identified clashes were resolved through the iterative model adjustments including duct rerouting and support geometry modifications, ensuring a suitable constructability. The final validated interference free assembly was subsequently rendered, which is suitable for high-fidelity meshing, establishing a robust framework for subsequent load simulation stages. Figure 6 shows the final model interferences free with the preprocessing of geometric structures. Special attention was given to the tendon profile ducts intersections and the anchorage zones. A minimum clearance of about 8 mm was maintained between the ducts and the adjacent reinforcement paths. Clash detection (interference test) was run iteratively for any overlap detection and was corrected by modifying duct routing or by adjusting the segment geometry as per requirement to ensure a constructible and analysis ready model free of any internal conflicts.

2.5. Meshing and Applying Boundary Conditions (Applying Loads)

Meshing is basically the discretization of the model structure which involves dividing or breaking the entire geometric entity into smaller finite elements which can accurately apprehend the structural behavior under the loading conditions during the simulation analysis. Figure 7 shows the refined meshing method carried out for the modelled structure.

A refined meshing strategy is implemented for partitioning the validated/preprocessed geometry into hexahedral elements with a strategic refinement at the critical zones. The element mesh sizing followed a graduated protocol with the program controlled mechanical geometry settings for the segment joints, tendon bars and the temporary support reactions (interfaces, transitioning to 100mm elements in bulk concrete regions). Dead loads (DL) were auto generated through the gravity activation setting synchronized with a sequential segment placement while superimposed dead loads (SIDL), including form traveler reactions and equipment loads, were applied as surface pressures at the corresponding construction phases.

2.6. Governing Equations

The finite element analysis is based on some standard and governing equation (2) of the structural mechanics by incorporating the linear elastic behavior with localized nonlinear effects at the connections and the supports. The fundamental FEA formulation is expressed as follow:

$$[K]\{u\}=\{F\} \quad (2)$$

Where,

[K] = global stiffness matrix assembled from element contributions.

{u} = nodal displacement vector

{F} = global load vector representing DL and SIDL during staged construction.

These theoretical considerations formed the basis of the simulation analysis ensuring both numerical accuracy and compliance with the codal provisions. Further the constitutive relationship for concrete and steel in the elastic limit is given in equation (3) and equation (4) below:

$$\sigma_c = E_c \times \varepsilon_c \quad (3)$$

$$\sigma_s = E_s \times \varepsilon_s \quad (4)$$

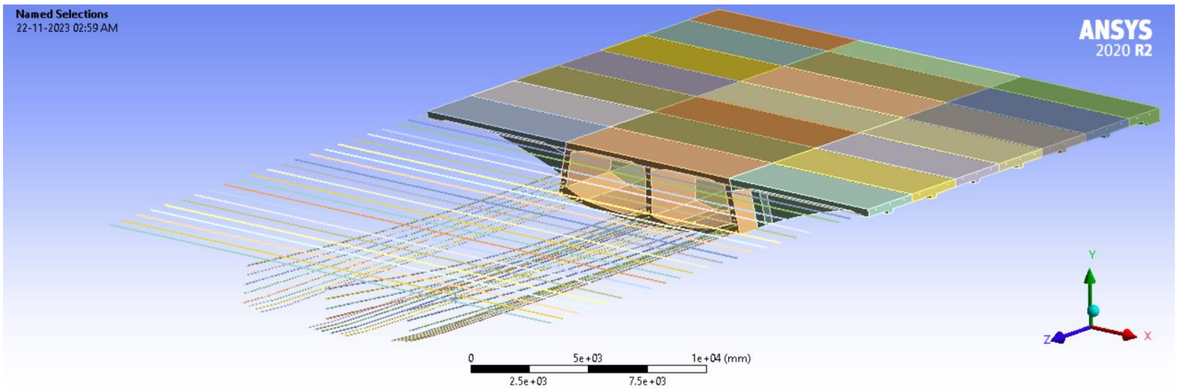

Figure 6. Interference Free 3D Geometric Modelled Structure

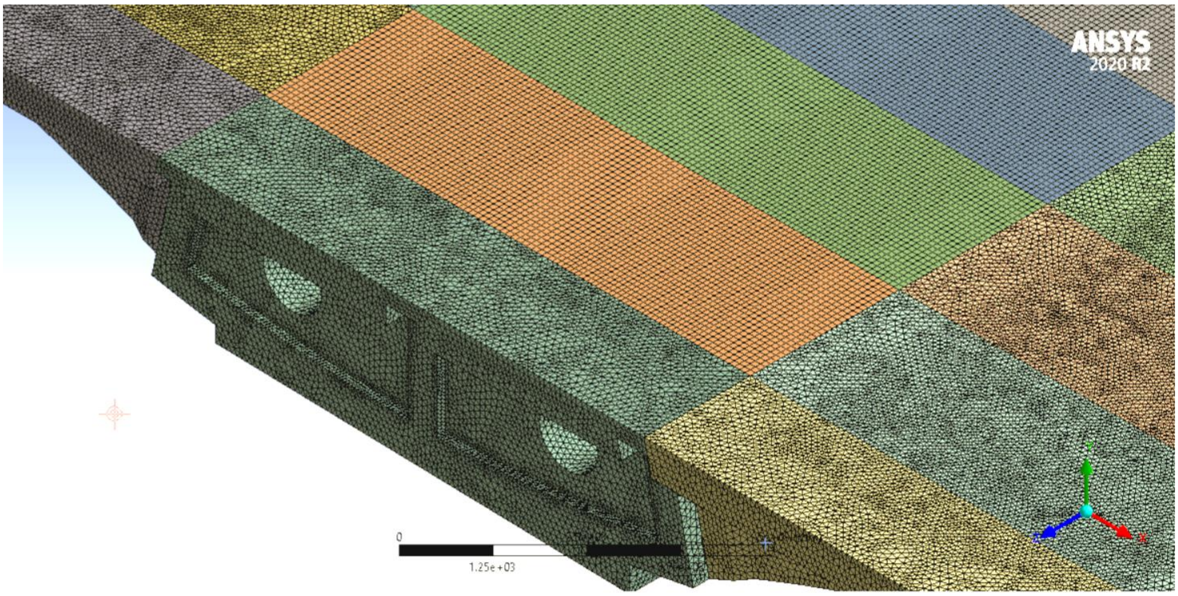

Figure 7. Refined Meshing Method for the Modelled Structure

3. Results and Discussion

This section is for the detailed discussions of the results so generated by solving the analysis carried out so far in line to the methodology conceptualized for the analysis of the structural elements. This phase involves interpretation of the outcomes of structural analysis to know the bridge performance under the applied loads and boundary conditions.

3.1. Deformation

The study further focuses on the stress concentration on the bridge entities. Figure 8 illustrates the deformation pattern/behavior of all the segmental entities of the spine and wing type box girder bridge under the applied loadings captured through finite element analysis. Subfigure 8(a) presents the full span view showing maximum displacement concentrated near the middle edge portion of the span indicating the primary flexural zone. Subfigure 8(b) focuses on all spine segments where deformation increases progressively towards the center part, highlighting the spine' critical role in resisting longitudinal bending moments. Subfigures 8(c) and 8(d) display the left and the right wing segments entities respectively, revealing asymmetric displacement patterns likely due to cantilever, torsional effects or eccentric loadings. As per visuals the maximum deformation in wing segments is localized and seems less severe than in the spine, confirming their secondary yet essential contribution to overall stiffness and the deck stability. This visual output supports the identification of high-stress zones and helps in optimizing segment geometry and reinforcement detailing.

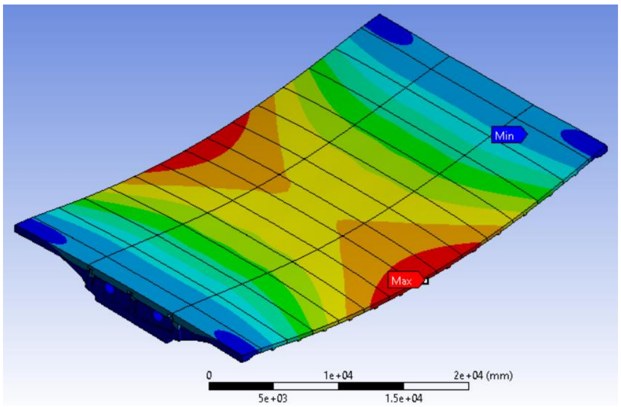

(a) Full Span

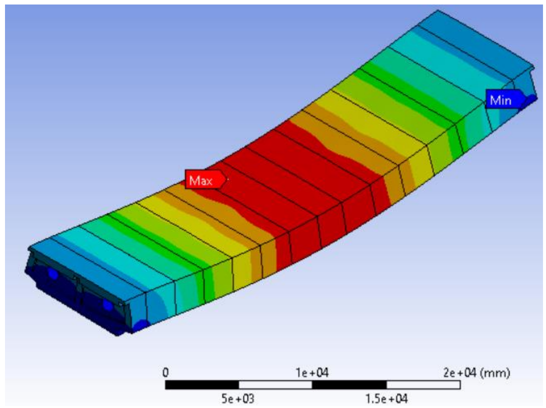

(b) All Spine Segments

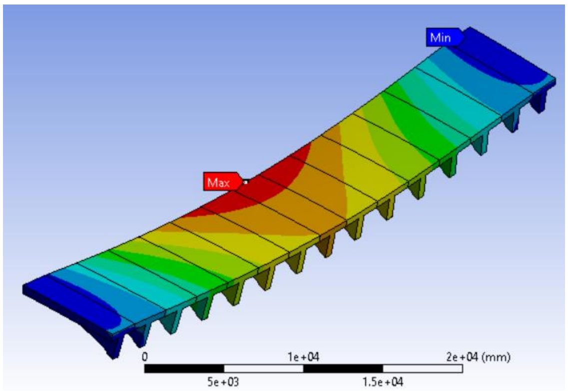

(c) LHS Side Wing Segments

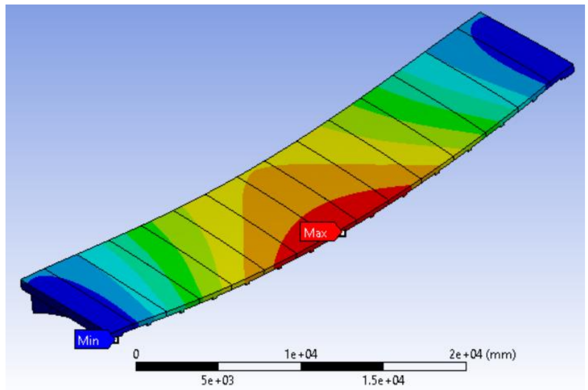

(d) RHS Side Wing Segments

Figure 8. Segment Body Entities

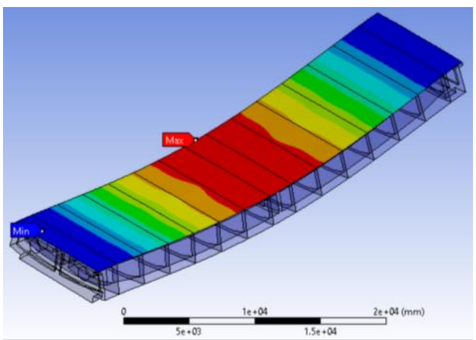

(a) Spine Top Face

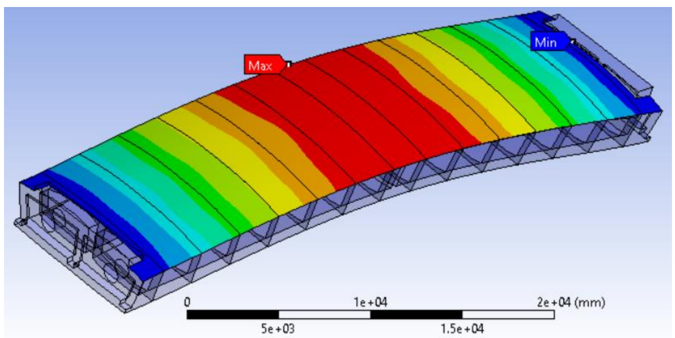

(b) Spine Soffit Face

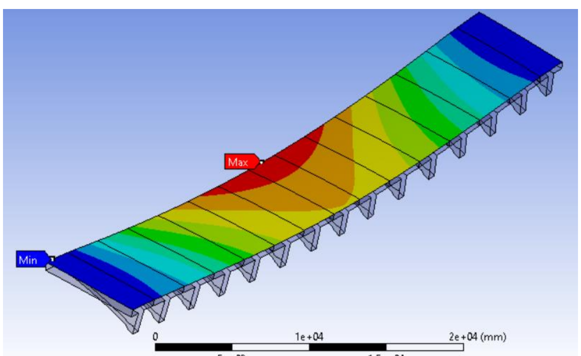

(c) Wing Top Face

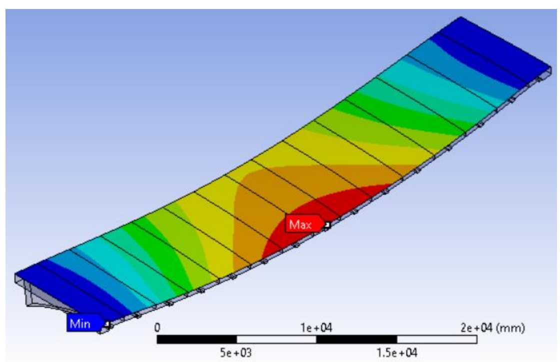

(d) Wing Soffit Face

Figure 9. Segment Face Entities

Similarly, Figure 9 reflects the behavior across selected segment face entities of the box girder bridge focusing on both the spine and wing faces. Subfigures (a) and (b) show the top and soffit faces of the spine element respectively. Subfigures (c) and (d) illustrate the top faces of the wing segments for left and right hand sides showing similar curvature driven displacement patterns. These face wise evaluations help in pinpointing zones of critical stress concentration and guide the refinement of reinforcement and prestressing layouts for both top compression zones and bottom tension regions.

Further the Table 1 represents the total deformation values (in mm) observed in various structural entities of the segmental box girder bridge structure, correlating with the displacement contours shown in Figures 8 and 9. These values represent maximum vertical deformations under the applied loads and help to assess the deformation behavior of different parts of the bridge structure.

Table 1. Total Deformation Values

Entities	Deformation Values (mm)
Full Span	19.222
All Spine Segments	15.249
All Wing Segments LHS Side	19.143
All Wing Segments RHS Side	19.222
Spine Segments Top Face	15.143
Wing Segments Top Face LHS Side	19.143
Wing Segments Top Face RHS Side	19.222
Spine Segments Bottom Face	15.249

The full span and wing segments on RHS side reflect the highest deformation value which is around 19.2 mm. This max deformation of the wing segments is expected due to their extended cantilever geometry. The spine segments show less deformation compared to that of wings, which is about 15.2 mm, indicating that the central spine entities offer more stiffness and the structural stability. When looking at individual faces for the top and bottom surfaces of the spine, it remains fairly consistent in their behavior, while the wing top faces reflect similar deformation values to their corresponding full segment parts. These observations match the patterns shown in Figures 8 and 9 and help confirm that the bridge responds primarily through expected bending behavior with the wing entities showing more flexibility than the spine segments.

Figure 10 illustrates the segment wise total deformation distribution across all the 15 spine entities of the segmental box girder bridge structure. The graph shows a symmetric parabolic trend typically the flexural behavior under uniform or symmetric loading conditions. The deformation value starts from a minimum of 3.19mm at both end segments S1 and S15, which is increasing gradually towards the S8 segment, where it reaches a peak deformation having a value of 15.249mm which lies at the center of the span. The Segments S6 to S10 show the max deformation zone with the values exceeding 14mm indicating the critical region subjected to maximum bending. While moving away from the center towards the supports, the deformation value decreases symmetrically. This behaviour pattern confirms that the spine behaves like a simply supported or continuous beam where the bending induced deflection is highest at the midspan and is least near the supports. Figure 10 validates the expected flexural response of the structure and it helps in identifying the segments where reinforcement detailing and prestressing should be critically optimized as per requirements.

A similar pattern for the wing segments is observed as shown in the Figure 11 where the total deformation is across the right side of the wing segments W1 – W15. The deformation starts at 3.18mm at both ends further increasing gradually towards the center portion reaching its maximum value of 19.22mm at the segment W8. This trend confirms that the wing segments also experience the peak bending near midspan due to flexural loading similar to that observed for the spine segments. The parallelled deformation pattern across the spine and wing entities indicates a well-balanced structural response and validates the accuracy of the segmental bridge model under the loading conditions considered.

Figure 12 represents the directional deformation along the Z-axis focusing on a specific section of longitudinal deformation along the bridge. The contour indicates both positive and negative directional movements along the span with values ranging from a maximum of +3.0561 mm to a minimum of -3.0558mm. This gives insights into a bidirectional displacement likely due to localized bending or rotation in the component under applied loads. The color gradient from across the cross-section of the structure also confirms stress reversal or an alternating deflection which is critical for the fatigue prone regions. The deformed shape also suggests that some interface occurs due to slip or warping which is often expected at construction joints or the connections between precast segments. This visualization is crucial for checking the stiffness along the span in z-direction for the joint stability and for refining the reinforcement detailed in critical zones like bearings, diaphragms or tendon anchor blocks where the directional displacements can influence the performance and the long-term durability of the bridge structure.

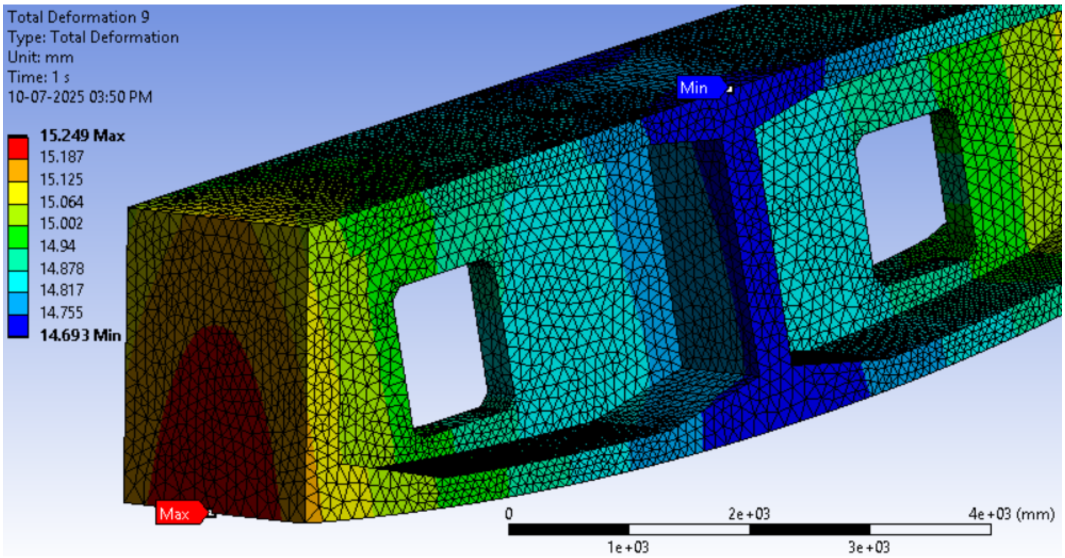

(a) Spine Max Deformations

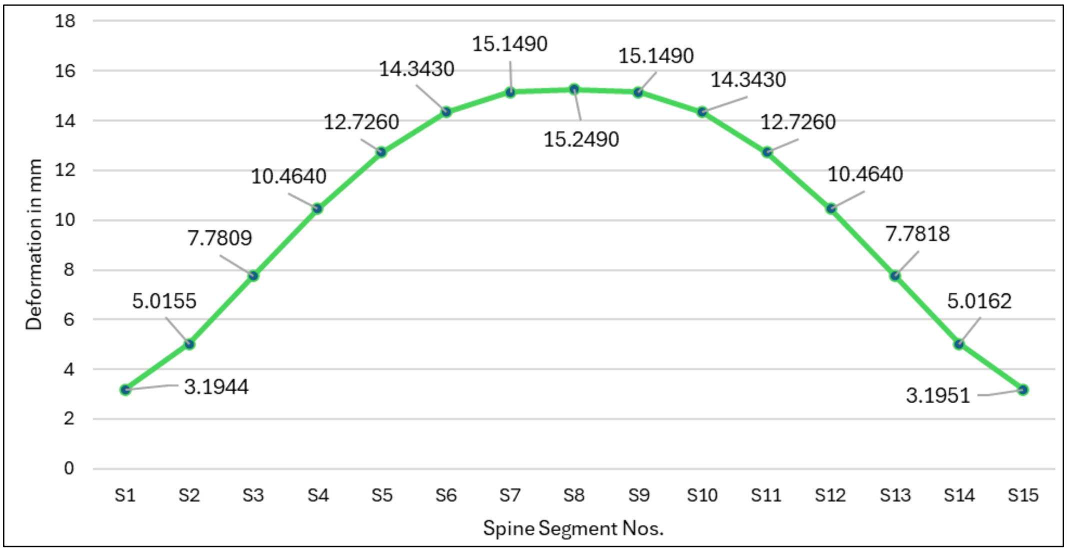

(b) Spine Deformation Curve

Figure 10. Segment wise Deformation for the Spine Segments

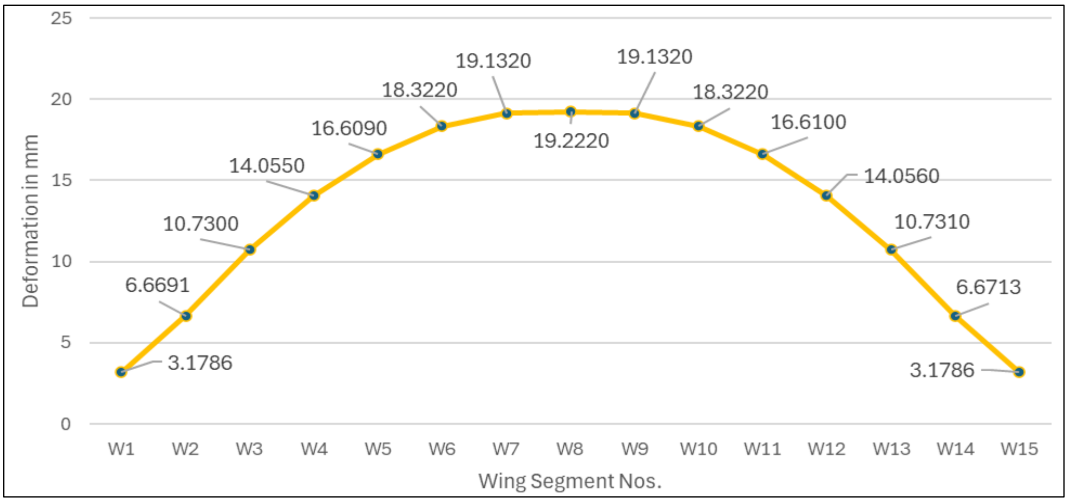

(a) Wings Deformations Curve

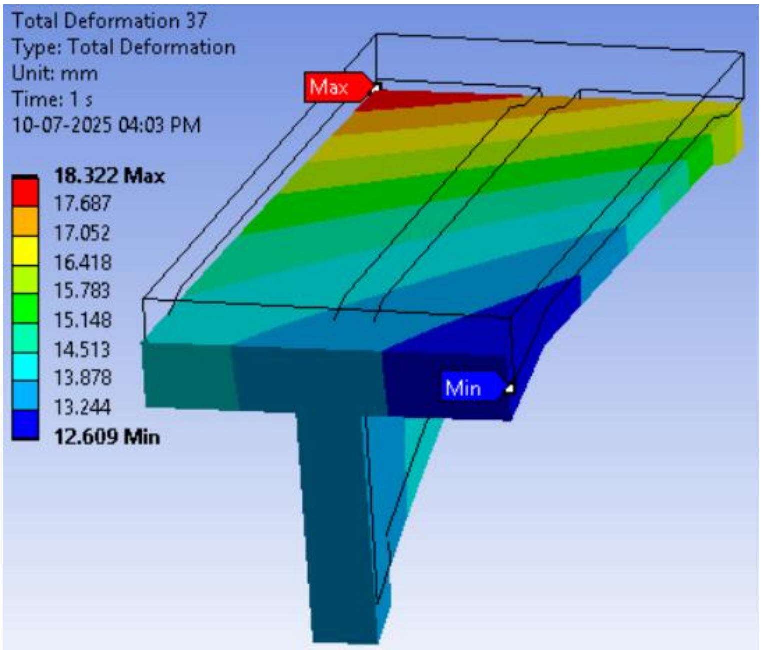

(b) Wing Max Deformations

Figure 11. Segment wise Deformation for the Wing Segments

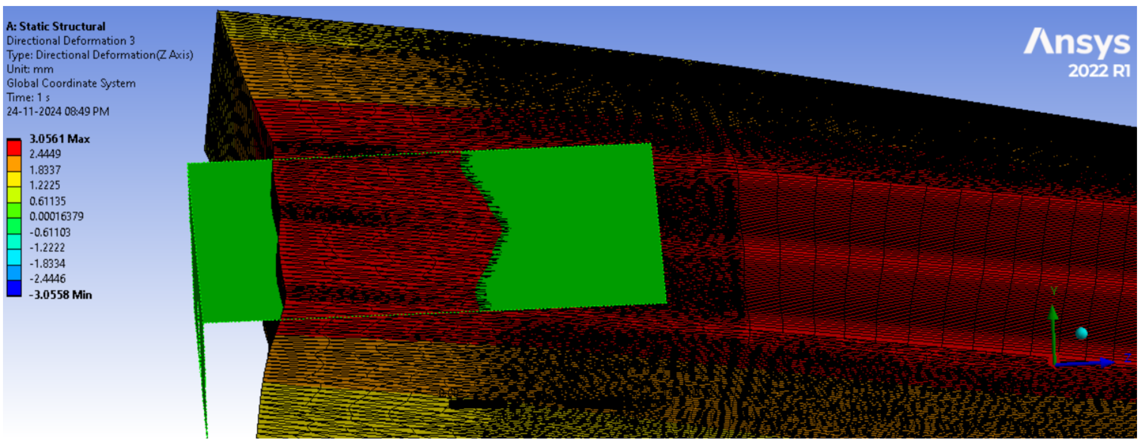

Figure 12. Directional Deformations

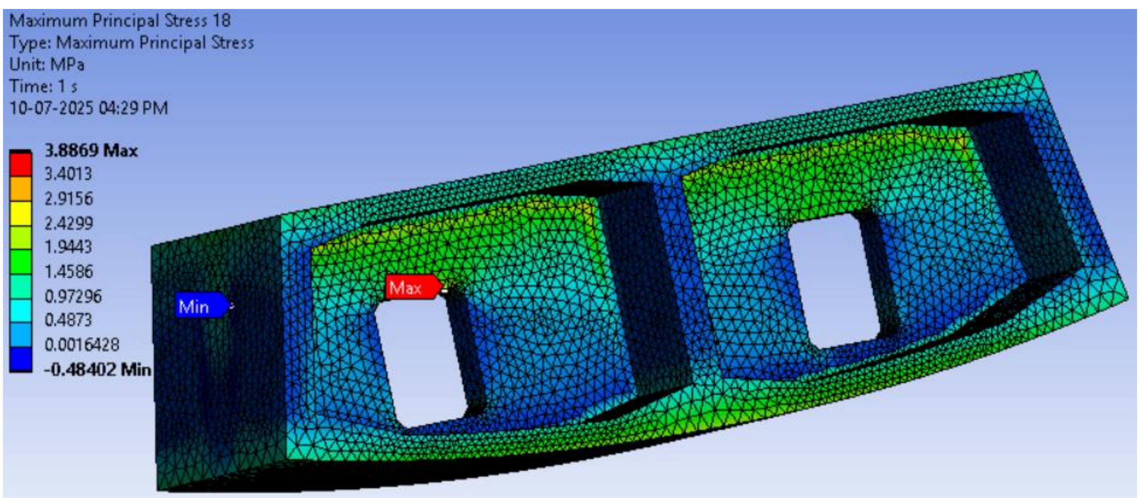

(a) S8 Central Segment

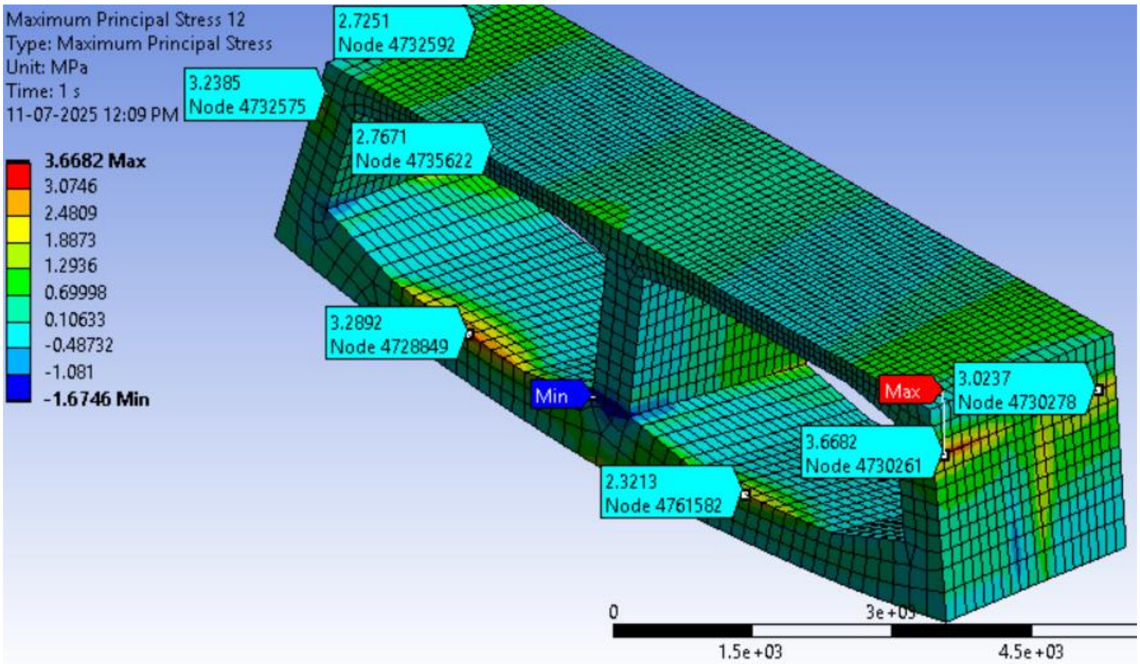

(b) S2 Segment next to DS Segment

Figure 13. Maximum Principal Stress Spine Segment

3.2. The Stresses

The study further focuses on the stress concentration on the bridge entities. Figure 13 shows the maximum principal stress distribution of spine segment S8 of the bridge evaluated through the finite element analysis. The stress values measured in megapascals (MPa) range from a minimum value of -0.48 MPa to the maximum of 3.89 MPa where the negative value indicates the tensile stress while the positive value indicates compressive stresses. The highest tensile stress is observed near the corner edge of the internal diaphragm cutout which is a region likely to experience a local concentration of stress due to geometric discontinuity and twisting/bending effects. The outer webs, top slab and soffit of the segment show moderate to low stress zones. This stress pattern indicates that the structure is behaving as expected under the flexural loading conditions with the critical tension zones developing where stress flow is interrupted by an opening. The overall stress remains well within the permissible range for M60 grade concrete confirming to the safe performance under service loads.

The maximum stress reaches 3.67 MPa at an outer web-slab intersection for the S2 segment, which is near or next to the supporting Diaphragm Segment (DS). Conversely the minimum value of –1.675 MPa suggests a localized tensile stress at the base of the middle web. Other nodes along the diaphragm show stress levels ranging from 2.3 MPa to 3.2 MPa with a generally uniform distribution across the slab region but elevated values near corners and cutouts. Figure 14 illustrates the maximum principal stress distribution for the wing segments of the box type bridge structure, highlighting a localized stress concentration near the free edge of the cantilever portion.

The maximum principal stress recorded is 5.68 MPa occurring at the junction of the web of wing coinciding with the spine side face. This region experiences a higher tensile stress of -2.64 MPa due to the cantilever action and torsional effects from the eccentric loading. The close-up view confirms that the stress value peaks sharply near the geometric transition, while the rest of the wing area remains in a lower stress range, which is mostly under 3 MPa. However, due to its localized nature reinforcement detailed in this region must be carefully checked to prevent early cracking or the long term durability concerns.

Figure 15 shows the stress values at all the key faces for spine segments at the top and bottom sides along the bridge structure. As from the subfigure 15(a) the top face of spine segment shows a mild stress value of about 3.13 MPa in compression and -0.76MPa in tension which is indicating stable under flexure. However subfigure 15(b) reveals significantly higher stress values on the bottom face of spine segments particularly near the bearing wedge zone, where the compressive stress reaches a value of 25.38 Mpa, and tensile stress goes to -15.86 MPa. This highlights a critical area of stress concentration that occurs likely due to the bearing reaction forces and end restraint.

Additionally the stress value is checked for the faces of the support which is coming around to be the maximum stress of 74.36 MPa and -10.81 MPa at support A, while the value is nearly same for the support B which is around 69.15 MPa and -9.37 MPa in the compression and tension respectively. These values indicate that peak stress values occur at the support interface sections particularly in the anchorage zones demanding enhanced and watchful detailing of the reinforcement to avoid any localized cracking or the long term fatigue issues.

Figure 16 shows the variation of maximum principal stress across all the spine segments from S1 to S15 of the bridge structure clearly indicating the critical zones near support. The S1 and S15 are the support segments also called as the Pier segments or the Diaphragm Segments (DS). The highest stress values are observed at the S1 segment about 25.39 MPa and the S15 segment about 25.21 MPa located at the support regions where concentrated bearing loads induce peak stress values. The central segments particularly S7 to S9 exhibit much lower stress levels with a maximum of only 3.89 MPa at the segment S8 reflecting a uniform flexural behavior away from the supports. This distribution confirms that while the midspan remains structurally stable under service loads, the end segments require a detailed stress management, including an enhanced reinforcement and possible confinement needed to prevent an overstressing and to ensure longer structural durability.

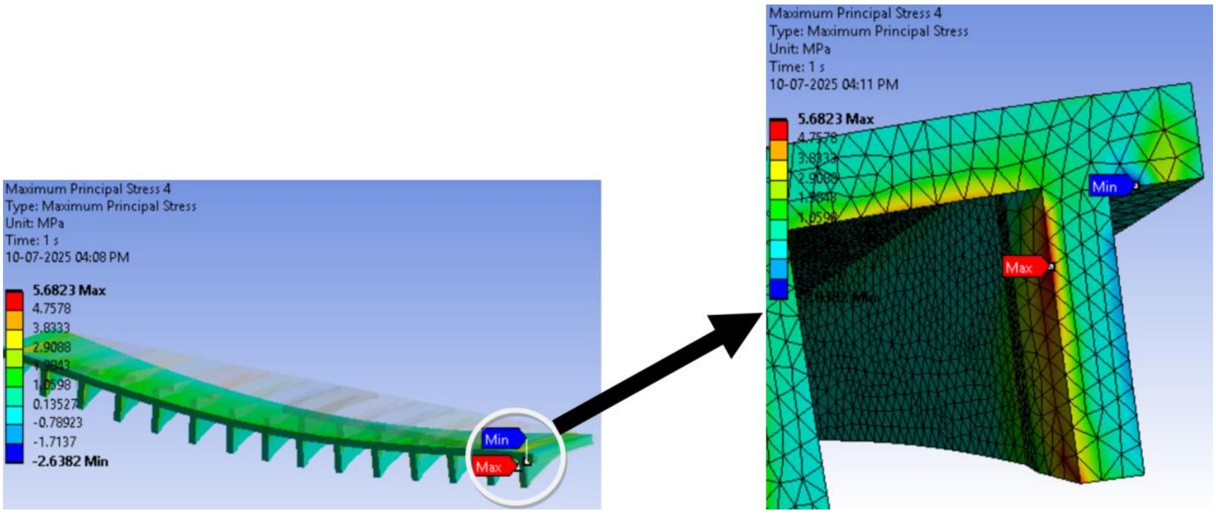

Figure 14. Maximum Principal Stress of the Wing Segments

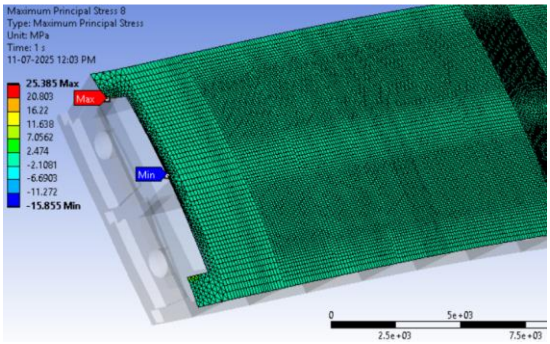

(a) Spine Top Face

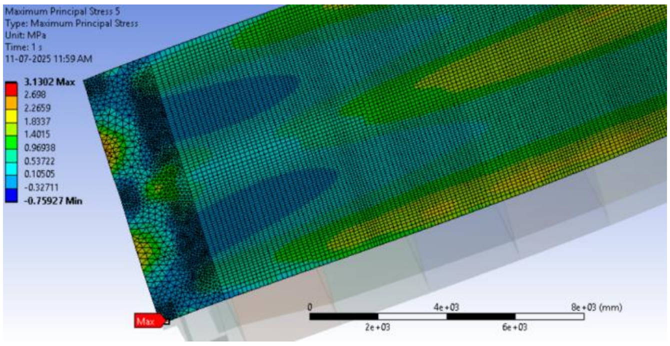

(b) Spine Bottom Face

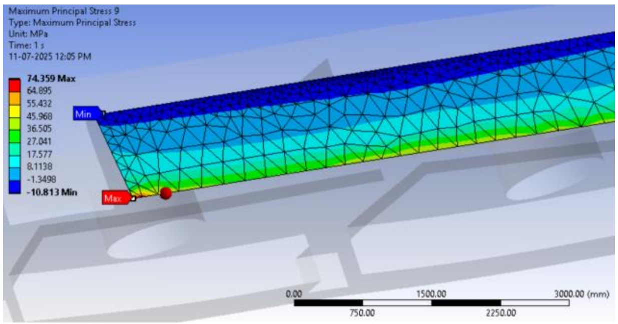

(c) Support A Face

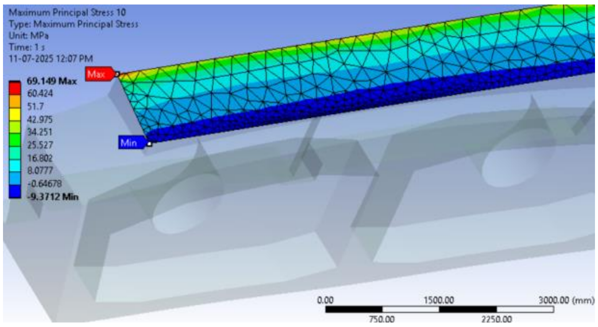

(d) Support B Face

Figure 15. Maximum Principal Stress at Spine and Wing Faces

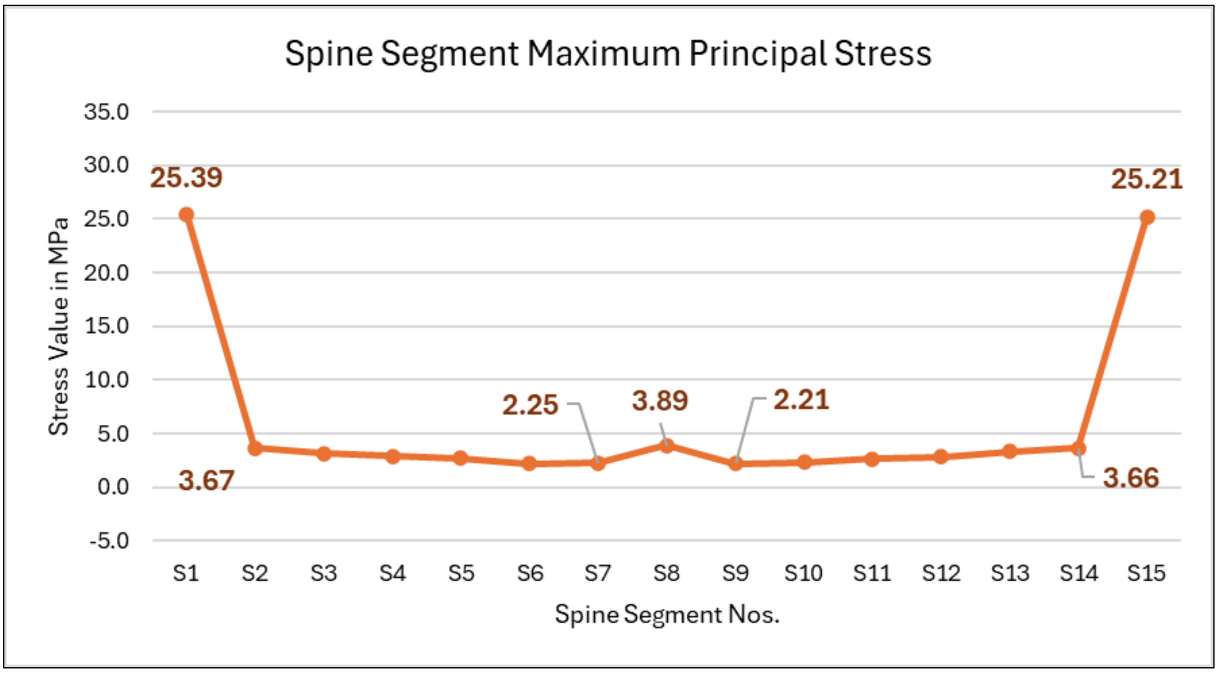

Figure 16. Segment Wise Maximum Principal Stresses

For the stress concentration in the cantilever portion, Figure 17 compares the maximum principal stress distribution across the left and right wing segments of the bridge structure numbered from L-W1 to L-W15 and from R-W1 to R-W15, respectively. In both graphs the stress pattern follows a symmetrical U-shaped curve with the higher stresses concentrated at the ends near support and lower stresses near the midspan during the construction phase. The left wing stress value peaks at 6.84 MPa at L-W1 and 6.03 MPa at L-W15 while the minimum value of 2.04 MPa is observed around L-W8 segments. Similarly for the right wing segments the maximum stresses of 5.68 MPa at R-W1 and 5.60 MPa at R-W15 decrease towards the center with a low value of 2.45 MPa at R-W8 segments. These trends of curve clearly reflect a typical cantilever behavior where the stress intensifies near the supports due to bending. The relative behavior on both sides suggests a structurally symmetrical response of the structure under the loading, although a slightly higher values on the left wing may indicate minor eccentricity or load imbalance due to one side slope/camber. According to the revised IRC:112-2020, the maximum permissible stresses in concrete shall be under the rare combinations of loads limited to 0.48 fck.

The limiting concrete stress under service load conditions for uncracked sections is 0.48 × fck, where fck is of concrete. For M55 grade concrete the characteristic compressive strength is 55Mpa and the max permissible stress in the concrete is 0.48 times of 55 which is around 26.4 MPa. This indicates that the section is structurally safe under the given service load conditions, and no additional reinforcement or redesign is necessary based on stress criteria alone. The results confirm that the structure is performing well within allowable limits, ensuring durability and crack resistance as per the latest code provisions.

3.3. The Strain

The results and discussion are based on the strain parameters. Figure 18 shows the maximum principal elastic strain values recorded at the locations of the entities shown in Figure 8 and 9 with respect to the body entities and face entities of the bridge structure. The highest strain value observed in the span for the spine segment is 0.0024, which is at the support segment S15 regions, while the S1 support segment shows relatively lower strain value of 0.00225 due to flexural action. The wing top face on the LH side also shows a notable strain of 0.00013 while for the RH side the strain value is 0.00012. This value of wing strain is much lower compared to that of strain occurring in the spine segments.

The distribution of the maximum principal elastic strain across different structural entities like spine segments, wing segments, top/bottom faces and the supports shows a notable variation, ranging from 0.000118 to 0.0024. High Strain values in spine and wing top faces are due to the concentration of the prestressing forces at transfer load conditions. Mesh refinement was applied in these regions to capture the localized stress concentrations which led to the higher strain values compared with bulk concrete regions. The strain values remain well within permissible limits prescribed by IRC:112 confirming that the structural responses during construction stages are safe and consistent with the expected behavior.

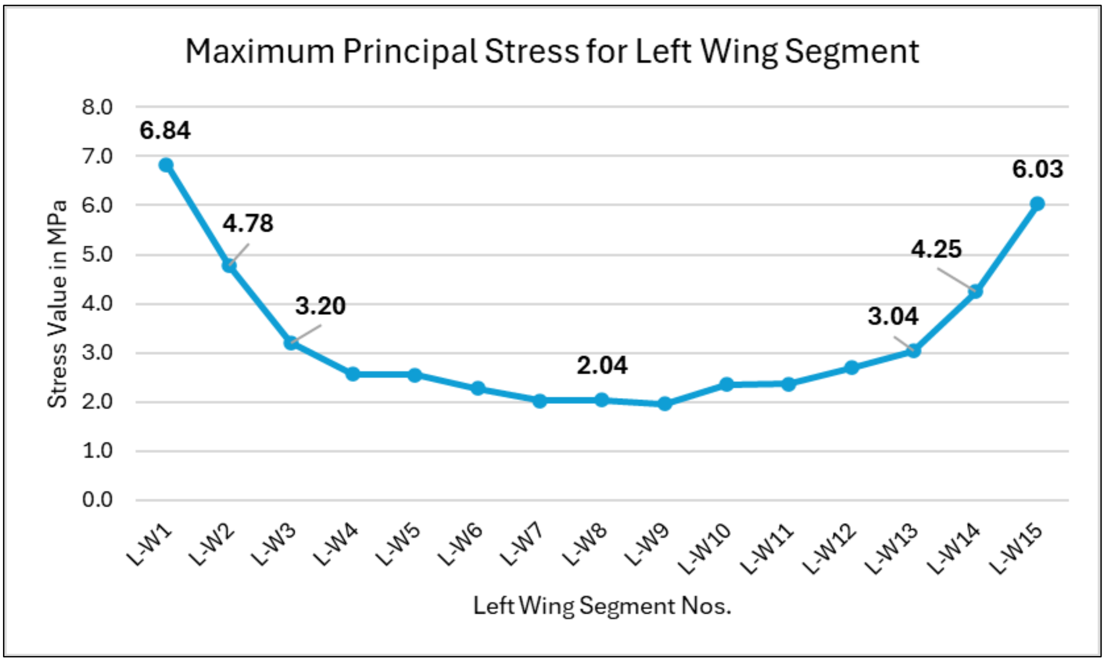

(a) LHS Wing Segments

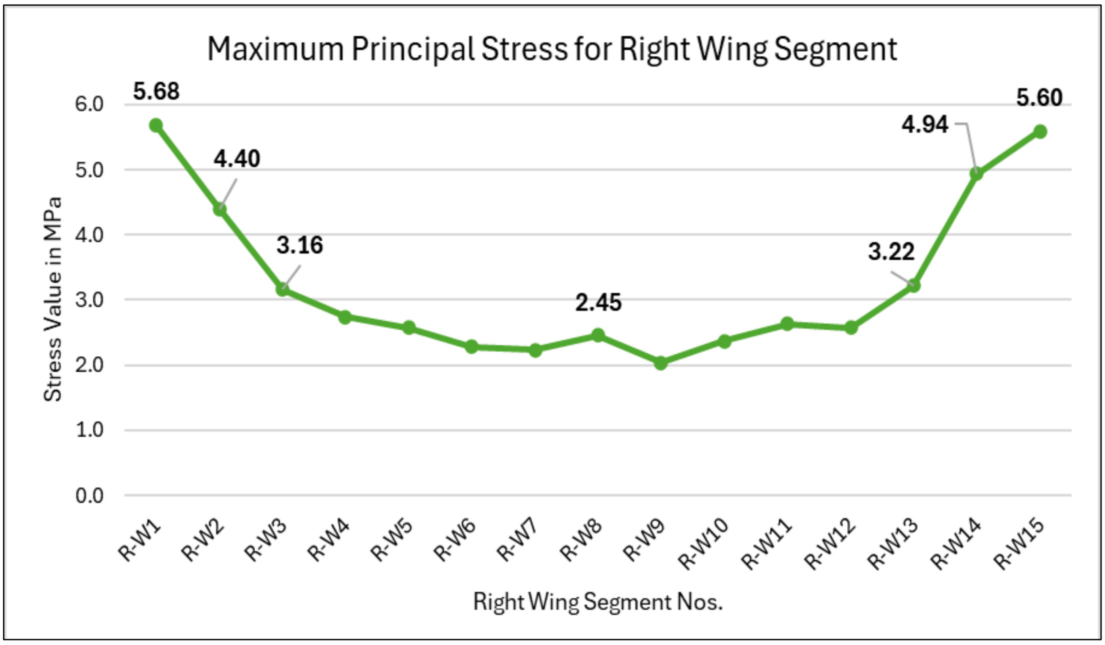

(b) RHS Wing Segments

Figure 17. Maximum Principal Stress of Wing Segments

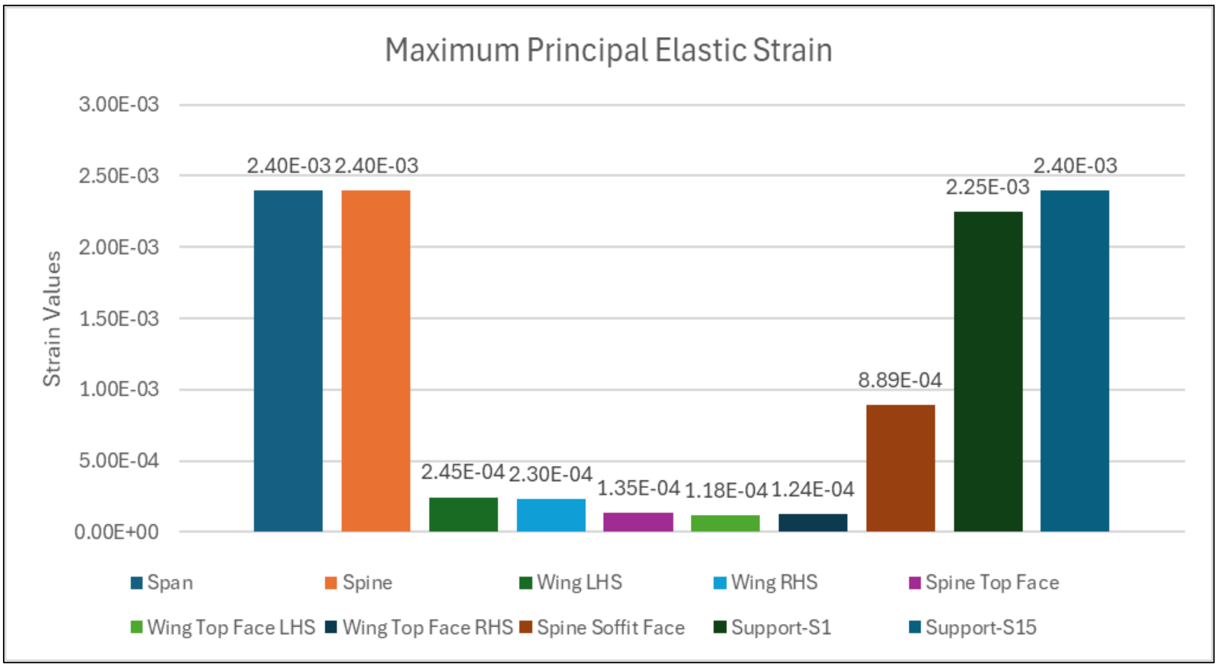

Figure 18. Maximum Principal Elastic Strain

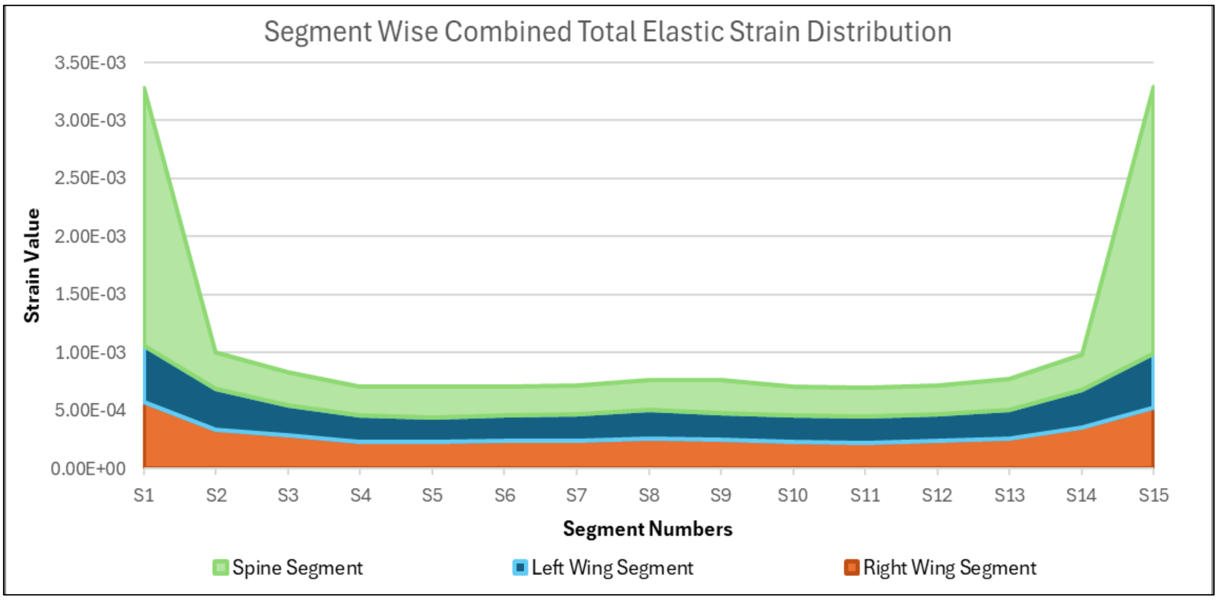

Figure 19. Total Elastic Strain Distribution Combined for All Segments

The contribution from the LH and RH wing segments remains consistent across all the segments with a slightly elevated value near the ends aligning with the deformation patterns observed in the previous Figure 19. Overall this distribution confirms that strain demand is most critical at segment extremities which is emphasizing the need for enhanced reinforcement detailing and the crack control measures to be taken in those specific regions for the long term durability and serviceability of the bridge structure. To ensure the reliability of the numerical simulation data the obtained results are compared with the codal provisions specified in IRC:6 and IRC:112 [21,22]. The maximum deflection across the span was found to be 19.22 mm, which is well within the permissible serviceability limit of Span/800 (50 mm for a 40 m span). Similarly the maximum principal stress in the spine segment observed to be 25.38 MPa at support S1 and 25.21 MPa at support S15 remains below the allowable stress limit of 0.48 fck, which is 26.4 MPa for M55 grade concrete, and this also confirms that the modeled stress values conform to the codal requirements. Further for the strain based evaluation results also align with the IRC:112 limit of the ultimate compressive strain of 0.0035 while the initial tensile strain thresholds at 0.0001–0.0002 are realistically captured in the simulation analysis. These comparisons substantiate that the numerical analysis findings are consistent with established design codes thereby providing codal validation to the present study.

3.4. Limitations and Future Scope

This study is limited to the linear elastic limits and the finite element simulations of precast segmental bridge components during the staged construction. The effects of creep, shrinkage, temperature variations and the long term prestressing losses were not explicitly analyzed as per IRC 18 [23]. Similarly the dynamic effects such as seismic loading, vehicle induced vibrations and impact loads were beyond the present scope of analysis. The validation was carried out through the code based checks, however direct experimental or field monitoring data would further strengthen the reliability of the results. For future work the nonlinear material modeling and time dependent effects can be studied to capture the long term serviceability of the structure. The dynamic and seismic analyses under realistic loading conditions can also be performed to evaluate the structural resilience.

4. Conclusions

The structural performance evaluation of the PSC segmental box girder bridge reveals a well-defined behavior in terms of the parameters like deformation, stress, and strain distribution. The point wise observations concluding the present research are as follows:

- The maximum total deformation observed across the span is 19.22 mm, which remains well within the permissible deflection limits as per IRC:6-2017, which is Span/800 with the max permissible deflection and for a 40m long span is 50mm hence this ensures the structure is adequate for serviceability.
- The principal stress analysis highlights localized peaks particularly at the bearing zones where the stress values reach up to 74.36 MPa.
- The max principal stress observed for the spine segments is 25.38 Mpa at the support segment S1 in the spine region near bearings and 25.21 Mpa for the support segment S15. For M55 grade concrete the characteristic compressive strength is 55 Mpa and the max permissible stress in the concrete is 0.48 times of 55 which is around 26.4 Mpa. Hence the stresses are within the limit as per the IRC 112.
- By introducing state based parameters into the analysis framework, the study captures both compression and tensile behavior of the concrete more accurately while ensuring the compressive strength remains within the ultimate limit of 0.0035 as per the IRC:112. The framework also considers early tensile strength thresholds typically in the range of 0.0001 to 0.0002.
- The research introduced strain based parameters into the analytical framework shifting the focus from traditional stress- based evaluation to strain responsive behavior.
- By simulating the bridge response in real time the study enhances the predictive accuracy of dynamic performance helping engineers to better access critical conditions and make timely design for safety decisions.
- The study here along with its practical implications was aligned with the standard specifications and the guidelines prescribed in the MoRTH for road bridges, thereby ensuring the proposed methodology and the findings remain consistent with the national standards of design, safety and the quality of bridge structures.

REFERENCES

[1] Heggade V.N., "Evolution of Precast Segmental Technology for Bridges in India," Journal of the Indian Roads Congress. Paper No. 636. April-June-2015. https://www.researchgate.net/publication/355771100

[2] MORTH 2013 — "Specifications for Road and Bridge Works," Ministry of Road Transport and Highways, Fifth Revision, Indian Road Congress 2013, New-Delhi, India. https://law.resource.org/pub/in/bis/irc/mort.250.2013.pdf

[3] Heggade V.N., "Full span & segmental precast technology for Bridge superstructure," Indian Association of Structural Engineers, Course on Prestressed Concrete For Bridges & Buildings, March-May-2021. https://www.researchgate.net/publication/355493069

[4] Heggade V.N., "Construction-Centric Sustainability Of Precast Segmental Bridges Constructed With Span-By Span Method," The Bridge and Structural Engineers, Vol. 50, No. 4, pp. 82-96, September-December-2020. https://www.researchgate.net/publication/355486387

[5] Heggade V.N., "Avoidance of Collapses of Prestressed Concrete Elevated Structures & Bridges during Construction," 3-days Program for the Officers of MoRTH, NHAI, NHIDCL, BRO, IEs, AEs and Contractors in collaboration with National Highways Authority of India (NHAI), 23rd to 25th September 2021. https://www.researchgate.net/publication/355486875

[6] Heggade V.N., "Dimensional Scale Effects On Spine And Wing Bridges," The Bridge and Structural Engineers, Vol. 53, No. 1, pp. 65-86, March 2023. https://www.researchgate.net/publication/371120633

[7] Walter Padlony Jr., "An Overview of Precast Prestressed Segmental Bridges," Fedral Highway Administration, U.S. Departments of Transportation, PCI Journal, January-February-1979. https://doi.org/10.15554/pcij.01011979.56.87

[8] Yin, X., "Discussion on the construction quality control points of bridge concrete," SHS Web of Conferences, Vol.

158, ICPAHD 2022, p. 01007, 2023. https://doi.org/10.1051/shsconf/202315801007

[9] Razaqpur G. R., Nofal M., & Mirza M. S., "Nonlinear analysis of prestressed concrete box girder bridges under flexure," Canadian Journal of Civil Engineering, Vol. 16, No. 4, pp. 598–608, 2011. https://doi.org/10.1139/l89-127

[10] Suprajha G. S., Tamilarasan P., Balaji N., Sudarsan J. S., & Prasanna K., "Design and analysis of segmental bridge in India," AIP Conference Proceedings, Vol. 2277, No. 1, p. 020004, November 2020. https://doi.org/10.1063/5.0025304

[11] IRC:21-2000 — "Standard Specifications and Code of Practice for Road Bridges," Section-III, Third Revision, Indian Road Congress 2000, New Delhi, India. https://law.resource.org/pub/in/bis/irc/irc.gov.in.021.2000.pdf

[12] IRC:83-2018 — "Standard specifications and code of practice for road bridges," Section IX: Bearings (First Revision). Indian Roads Congress 2018, New-Delhi, India. https://law.resource.org/pub/in/bis/irc/irc.gov.in.083-3.2018.pdf

[13] Nan L., Yang Q., Liu Y., Meng X., Ye Y., & Sun Z., "Application of long-span continuous bridge technology in bridge construction," Journal of Architectural Research and Development, Vol. 7, No. 3, pp. 7-12, 2023. https://doi.org/10.26689/jard.v7i3.4827

[14] B. Pei, A. Chong, H. Xia & X. Kang, "Design and key construction technology of steel concrete steel sandwich composite pylon for a large span cable stayed bridge," Springer Scientific Reports, Vol. 13, p. 6626, 2023. https://doi.org/10.1038/s41598-023-33316-7

[15] Naik C. T., Achar M. M., & Lakshmi K., "Analysis and design of multi cell post-tensioned PSC box girder," IOSR Journal of Mechanical and Civil Engineering (IOSR-JMCE), Vol. 12, No. 4, pp. 56–64, July-August 2015. https://doi.org/10.9790/1684-12475664

[16] Barbosa A. F., & Ribeiro G. O., "Analysis of reinforced concrete structures using ANSYS nonlinear concrete model," Article in Computational Mechanics New Trends and Applications, Vol. 69, No. 5, pp. 457–471, June 1998. https://www.researchgate.net/publication/2584814

[17] N. R. Joshuva, S. Saibabu, P. E. Sakaria, K.N. Lakshmikandhan, P. Sivakumar, "Finite element analysis of reinforced and pre-tensioned concrete beams," International Journal of Emerging Technology and Advanced Engineering, Vol. 4, No. 10, October 2010. at: https://www.researchgate.net/publication/280737268

[18] Abbas S., Hameed A., Qazi A.U. and Nazir R., "Construction Stage Analysis Of Segmental Box Girder Bridge," Pakistan Journal of Science, Vol. 68, No. 4, December 2016. https://doi.org/10.57041/pjs.v68i3.205

[19] IRC:78-2014 — " Standard Specifications And Code Of Practice For Road Bridges," Section VII, Revised Edition, Indian Road Congress 2014, New-Delhi, India. https://law.resource.org/pub/in/bis/irc/irc.gov.in.078.2014.pdf

[20] IRC:SP:87-2019 — "Manual of Specification and Standards for Six Laning of Highways," Second Revision, Indian Road Congress 2019, New-Delhi, India. https://law.resource.org/pub/in/bis/irc/irc.gov.in.sp.087.2019.pdf

[21] IRC:6-2017 — "Standard Specifications and Code of Practice for Road Bridges," Section II Loads and Load Combinations, Seventh Revision, Indian Road Congress 2017. New-Delhi, India.https://law.resource.org/pub/in/bis/irc/irc.gov.in.006.2017.pdf

[22] IRC:112-2011 — "Code of Practice for Concrete Road Bridges," Indian Road Congress 2011. Reprinted June 2014, New-Delhi, India. https://law.resource.org/pub/in/bis/irc/irc.gov.in.112.2011.pdf

[23] IRC:18-2000 — "Design Criteria for Prestressed Concrete Road Bridges (Post-Tensioned Concrete)," Third Revision, Indian Road Congress 2000, New-Delhi, India. https://law.resource.org/pub/in/bis/irc/irc.gov.in.018.2000.pdf